A Laser-Induced-Fluorescence study on a cluster of two 100 W Hall thrusters

Clémence Royer, Stéphane Mazouffre, Alexis Lecervoisier

A Laser-Induced-Fluorescence study on a cluster of two 100 W Hall thrusters

IEPC-2024-790

Presented at the 38th International Electric Propulsion Conference, Toulouse, France
June 23-28, 2024

C. Royer* S. Mazouffre†
and A. Lecervoisier‡
ICARE-CNRS, France

Clustering offers multiple benefits compared to a single large thruster: a wider operating range since thrusters can be fired individually or in combination, a reduced cost due to the mass production of thrusters, an increased redundancy in case of a thruster failure, and enhanced thrust vectoring capabilities based on thruster arrangement. A significant operational factor is the physical interaction between the ion beam produced by each thruster. This interaction, which remains poorly understood, significantly affects thruster performance and the spacecraft environment. In this study, we experimentally investigate the interaction between the plasma plumes in a cluster of two 100 W xenon-fed Hall thrusters using Laser-Induced Fluorescence (LIF) spectroscopy on singly-charged metastable Xe^+ ions. These preliminary experiments clearly reveal plume overlap and ion invasion.

Nomenclature

$R_{e,Larmor}$	Electron Larmor radius
$L_{chamber}$	Thruster channel length
$\Delta\nu$	Doppler shift
ν	Laser frequency
ν_0	The frequency at rest
U_d	Discharge voltage
e	Elementary charge
M	Ion mass
$\lambda_{exc}(vac)$	Laser wavelenght in vacuum
$\lambda_{fluo}(air)$	Fluorescence light in air
Xe^+ or $XeII$	Singly-charged xenon ion
P_f	Final power density
α and β	Attenuation coefficient of lens and vacuum chamber window
P_{probed}	Probed power density
ϕ_{laser}	Beam diameter
r	Thruster internal radius.

*PhD candidate, clemence.royer@cnrs-orleans.fr
†Research director, stephane.mazouffre@cnrs-orleans.fr
‡Engineer, alexis.lecervoisier@cnrs-orleans.fr

I. Introduction

In recent times, the space industry has seen a remarkable rise in the demand for SmallSats and CubeSats. Projects like Starlink and OneWeb illustrate the growing trend towards deploying satellite constellations and miniaturizing systems. This development holds promise for advancing space exploration by lowering costs and reducing production timelines. The continuous technological advancements in the space industry and research sectors aim to expand human knowledge and operational reach. Key objectives for rocket scientists include launching more spacecraft to explore deeper into space, enhancing telecommunications networks, improving navigation systems, and fulfilling our relentless quest for discovery. To accomplish these goals, thrusters are crucial for maneuvers such as station-keeping, orbit transfers, and de-orbiting. Recently, cutting-edge electric propulsion systems have emerged as effective solutions for small satellite requirements.

Hall Thrusters (HTs), a form of ion thruster, have established their efficiency and reliability through numerous space missions over the years. Hall Thrusters, provides significant advantages in terms of thrust-to-power ratio, total impulse, and cost-effectiveness. Miniature Hall Thrusters are particularly effective for specific maneuvers like drag compensation or orbit correction for small satellites. The working principle of Hall Thrusters involves generating a magnetic barrier at the thruster exhaust using magnet rings or coils. Electrons emitted from an external cathode are affected by the magnetic field, which reduces their axial motion and causes them to drift azimuthally due to the ExB drift, generating the Hall current.

As illustrated in figure 1, propellant is injected into the thruster chamber near the anode region. When neutral atoms approach the magnetic barrier, they are ionized by collisions with electrons. These ions are then expelled from the chamber and accelerated to high velocities due to the potential difference. The magnetic field strength is carefully chosen to ensure that the electron Larmor radius is much smaller than the chamber length, $R_{e,Larmor} \ll L_{chamber}$, while preventing the excessive magnetization of the heavy ions.[2]

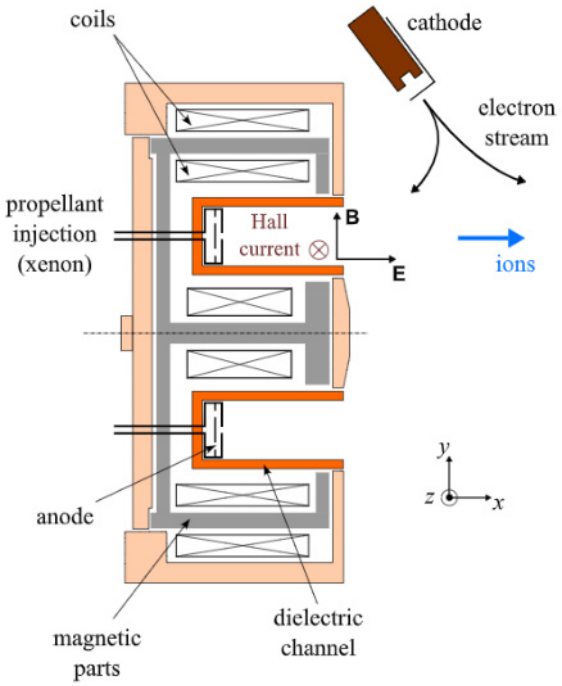

Figure 1: Cross section view of a Hall thruster

A pair of ISCT100 HT thrusters has been developed[5] to investigate the singularity of HT cluster system.[9] This research aims to characterize plasma plume interactions and determine the Velocity Distribution Function (VDF) of ions using laser spectroscopy. The experimental setup, including hardware and procedures, will be described in detail in the following sections of this paper. The saturation curve for a xenon-fed thruster configuration will be presented. Finally, we will examine the interaction between the plasma plume of the two thruster units by using xenon and krypton as both propellant and tracer gases.

II. Experimental diagnostic and set up

A. *LIF spectroscopy tool*

Laser-Induced Fluorescence (LIF) spectroscopy is a non-intrusive method used to measure ion velocity in various mode.[7] When the entire applied potential energy is converted into kinetic energy, the ion velocity is given by:[2]

$$V_{i,max} = \left(\frac{2eU_d}{M}\right)^{1/2} \tag{1}$$

Here, U_d represents the discharge voltage, e is the elementary charge, and M denotes the ion mass.

A laser beam is directed towards the thruster head along the channel axis in this experiment. The laser emits light at a specific wavelength to excite particles, causing a change in their energy levels. As the particles return to their original energy state, they emit photons, known as fluorescence light.[12]

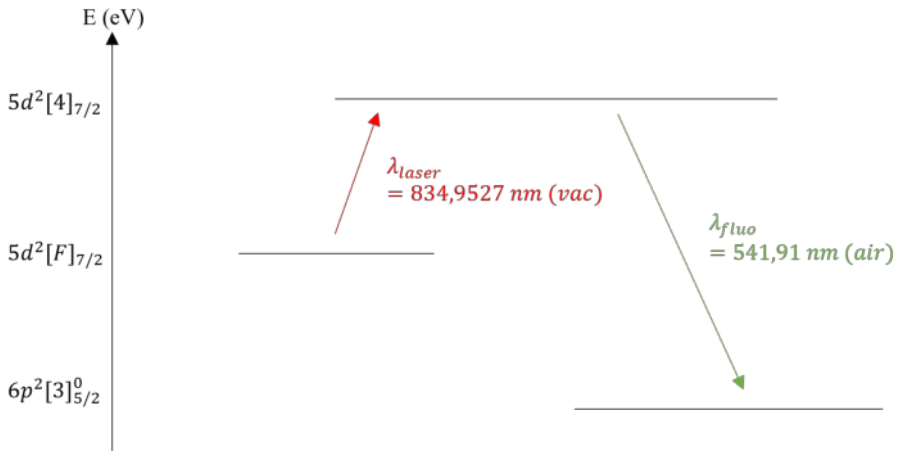

Figure 2: Energy diagram for LIF on metastable Xe^+ ions

For the metastable ion of interest in this study, the fluorescence photons fall within the green spectrum, while the applied laser beam is set in the near-infrared range, as shown in Figure 2. The ion velocity is determined by the Doppler shift of the optical transition as the Doppler broadening largely dominates the lineshape. Equation 2 provides the relationship between the laser beam wavelength and the ion velocity.

$$\Delta\nu = \nu - \nu_0 = \frac{1}{2\pi}\mathbf{k}\cdot\mathbf{v} \tag{2}$$

Here, $\Delta\nu$ represents the Doppler shift, ν is the observed frequency, ν_0 is the rest frequency, and v denotes the ion velocity. To determine the reference wavelength, table 1 lists ν_0 for each particle. In our study, we will probe metastable Xe II at the initial level $5d^2F_{7/2}$.

Table 1: Current excitation and fluorescence wavelengths in LIF studies on HTs.

Species	Initial level	$\lambda_{exc}(vac)$	$\lambda_{fluo}(air)$
Xe II	$5d^2F_{7/2}$	834.9527	541.91
Xe I	$6s[1/2]^o_2(1s2)$	834.9115	473.41

B. *Exprimental set up*

In this subsection, we introduce the optical bench setup. LIF measurements utilize a combination of devices to tune the red infrared laser beam. The laser beam is generated by a tunable laser diode capable of delivering 700 mW of power. With this laser diode, the wavelength can be varied from 810 nm to 840 nm, and the spectral width of the laser beam profile is approximately 1 MHz. During scanning over a specific laser frequency range, the beam light is continuously calibrated by a wavemeter with an accuracy of 80 MHz (approximately 60 m/s). Additionally, a scanning confocal Fabry-Perot interferometer with a 1 GHz free spectral range is essential for monitoring undesirable "mode hops" that could affect the laser quality.[11]

The primary laser beam is modulated by a mechanical chopper at a frequency of approximately 1 kHz before being passed through a half-wave plate and a polarizer to adjust the beam polarization if necessary. For all measurements in this study, the beam was vertically polarized. A schematic of the optical bench setup is shown in figure 3.

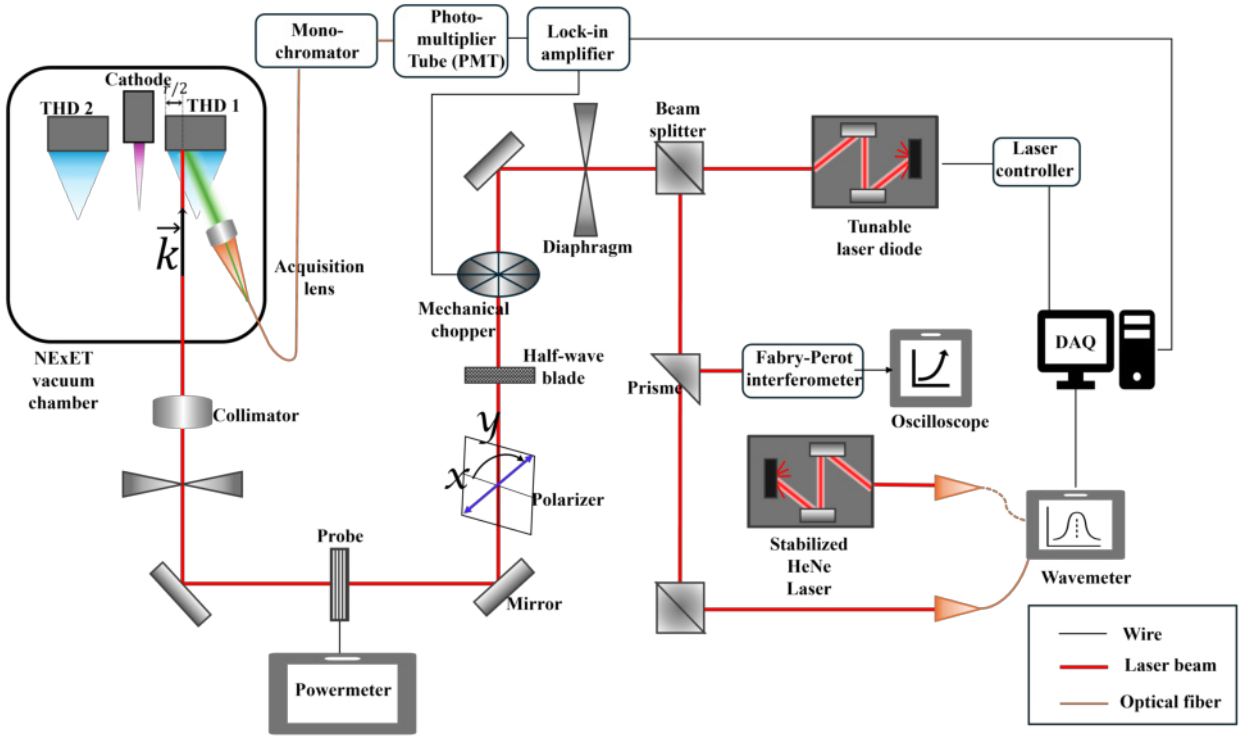

Figure 3: LIF set up schematic

The infrared laser is directed axially towards the plasma and aligned with the channel axis of one of the two thrusters in the cluster. This specific configuration allows for the determination of the axial velocity component of ions in the plume.

As depicted in figure 4, a lens is positioned directly inside the vacuum chamber beneath the cluster of two HT thrusters, with a focal length of 40 mm. It collects and transmits the fluorescence light through a 200 μm optical fiber. The fluorescence radiation obtained falls within the visible spectrum at a wavelength of λ_{fluo} = 541.91 nm. This value is set on a monochromator and remains constant throughout the experiment. The fluorescence light is filtered using a 20 cm focal length monochromator to isolate the fluorescence frequency from the rest of the spectrum. The acquisition point can be adjusted closer to or farther away from the HT exhaust area by utilizing two translation stages, as illustrated in figure 4.

For time-averaged LIF measurements, a lock-in amplifier operating at the chopper frequency is employed to distinguish the fluorescence light from the intrinsic plasma emission. The scanning of the laser diode cavity, data acquisition, and laser wavelength monitoring are all computer-controlled processes.

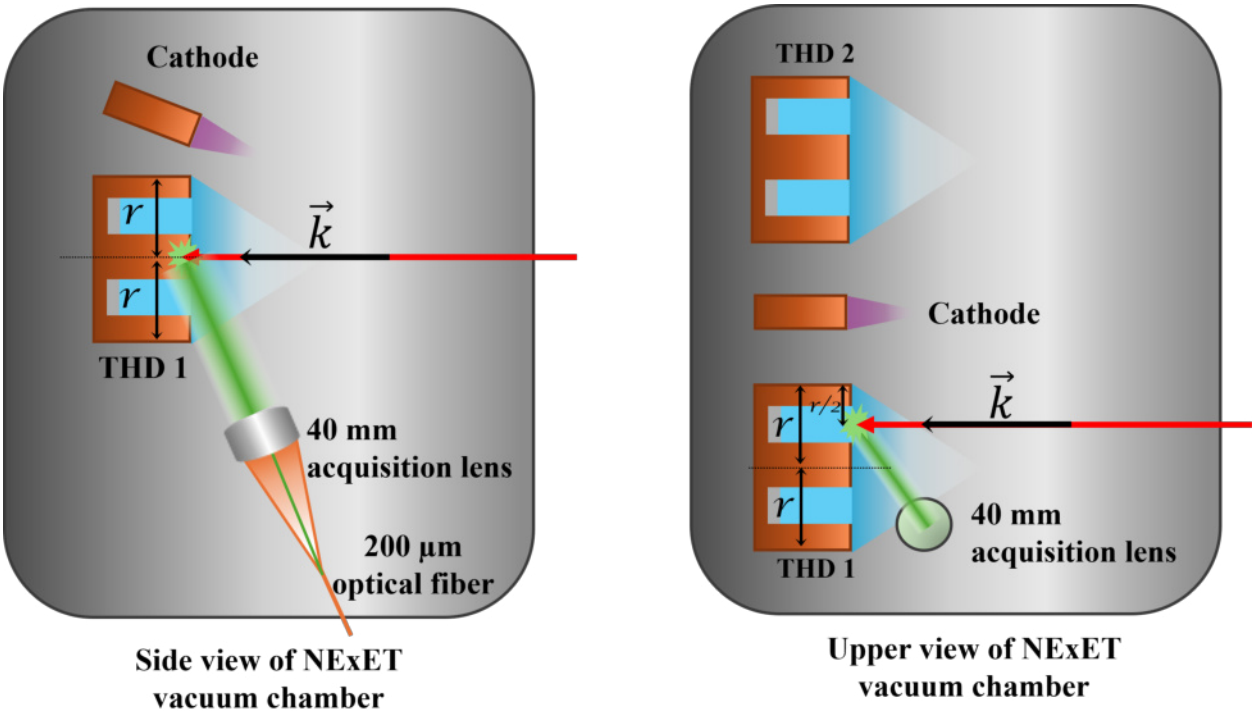

Figure 4: Layout of the experimental arrangement inside the vacuum tank.

Experiment layout, seen on figure 4, has been decided to identify plume invasion. Indeed, the red-infrared laser beam comes axially, right toward the THD1 inner side canal. This canal is the closest point to THD2 and is more likely to be exposed to plume interaction.

The fluidic system is illustrated in figure 5. A pair of mass flow controllers enables the transition between a fully xenon-fed system and a hybrid system incorporating both xenon and krypton. In the hybrid configuration, both thruster heads (THD) can be supplied with xenon or krypton. The remaining mass flow controller is responsible for delivering krypton to the cathode. During this study, it has been decided to use only krypton throughout the cathode in order to avoid any signal on IVDF profils coming from the cathode.

C. *Cluster configuration*

For our study purpose, a set of two identical 100 W-class ISCT100 Hall Thrusters have been installed on a frame inside the NExET vacuum chamber, at the CNRS-ICARE laboratory. Background pressure remains at 10^{-7} mbar whenever thrusters aren't firing, whereas pressure increases to 10^{-4} mbar when two thrusters

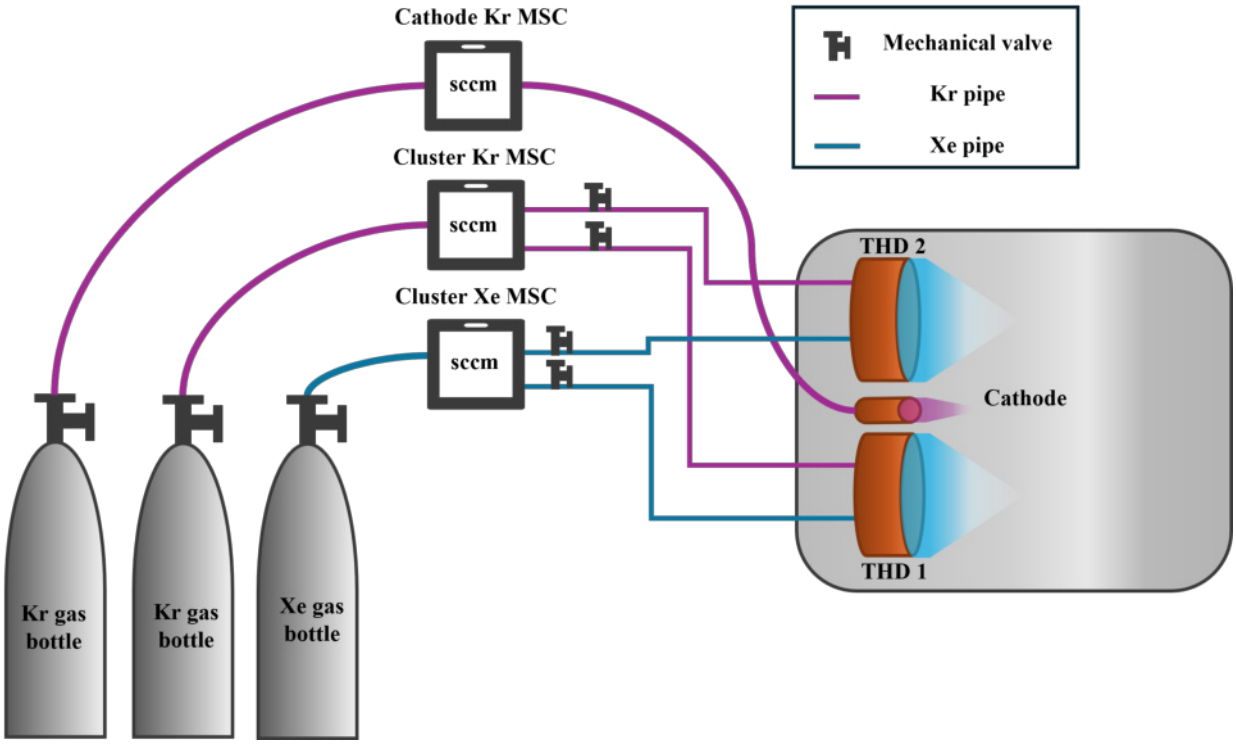

Figure 5: Vacuum chamber fluidic system schematic.

are simultaneously operated. A schematic of the set up and thruster assembly is depicted in figure 5.

Two power supplies have been employed to operate each thruster. The primary power supply is a Delta Elektronika device, which positively polarizes the anode of Thruster Head 1 (THD 1) and the common cathode keeper. The anode of THD 2 is supplied by another Delta Elektronica power supply. The discharge circuit is completed through the heater minus. When ignition is initiated, the potential switching of the keeper is deactivated. The operation point are developped in table 3.

The common cathode is a 5 A-class hollow cathode[1,10] featuring a LaB6 emitter and functions for cluster configurations.[3,6,13,14] The heater is continuously powered by a high-current EA-PSI power supply at 18A and 21V, with a power range varying from 360 W to 400 W. The conditions are specified in table 2.

Throughout the entire campaign, each thruster has operated at the same working point, with parameters detailed in table 2:

Table 2: Hollow cathode parameters.

Heater voltage limit [V]	Heater nominal applied current [A]	Maximum heater power [W]	Cathode Kr gas mass flow [sccm]	Heating process
23	18	380	2	The heater is gradually heated at 2 A/min speed

Table 3: Single Hall thruster parameters.

Stage	Applied discharge voltage [V]	Discharge current threshold [A]	Maximum HT power [W]	Anode mass flow [sccm]
Ignition	400	0.5	200	9
Operation	200	0.65	130	6 for Xe and 7 for Kr

Concerning the study parameters, we can determine the maximum velocity of Xe^+, assuming no energy loss. According to equation 1, this yields $V_{i,max,\infty} \approx 17.1$ km/s.

D. *Experimental conditions*

To lead this study, few cases have been examined. For all cases, LIF measurements have been performed at x = 10 mm along the channel axis of THD 1 (x = 0 mm refers to the exit plane). On the table 4, when "+" appeared next the gas reference, it means that the gas is being ionized and thruster is ON. If not, the thruster is OFF but gas is still injected through the chamber. The sign "-" indicates that no gas is supplied.

Table 4: Cluster operating conditions with a Kr gas supplied cathode.

Configuration number	HT1	HT2
0	-	-
1	Xe+	-
2	Xe+	Kr
3	Xe+	Kr+
4	Xe+	Xe
5	Xe+	Xe+
6	Xe	Kr+
7	Xe	Xe
8	Xe	Xe+
9	Kr+	Xe
10	Kr+	Xe+
11	-	Xe+
12	Kr+	-
13	Kr+	Kr
14	Xe	-
15	Xe	Kr
16	Kr	Xe
17	Kr	Xe+
18	-	Xe
19	-	Kr+

From the table4, we can see many experiments cases have been listed, however, only 10 of those conditions have been carried out. Experiment cases are presented the figure 6 and results will be shown and commented on figure 9, section III.
Among all those listed conditions, only ten have been tested : the case 1 and all cases from 3 to 11.
Configuration 1 is a good representation of a standard single thruster IVDF without any plume invasion and will be reliable profil to identify plume invasion consequences. This configuration is very similar to case 2, hence the condition 2 hasn't been performed.
The case 7, 12 to 16, case 18 and 19 are supposedly similar as the case 0 : absolutely no signal is expected. Therefore only one among those have been tested : case 7, remaining ones were unnecessary.
Finally, case 17 was considered as well unnecessary because of it similitude to the case 11.

On figure 6, when the plasma thruster is ON, it represents plasma being ionized in this case. The color is linked to the gas injected in the thruster head : violet for Kr gas and blue for Xe gas. Some photos present cases where thruster is OFF but gas is still injected in, regarding those cases, the gas name is just written at the place where the thruster head should normally appear.

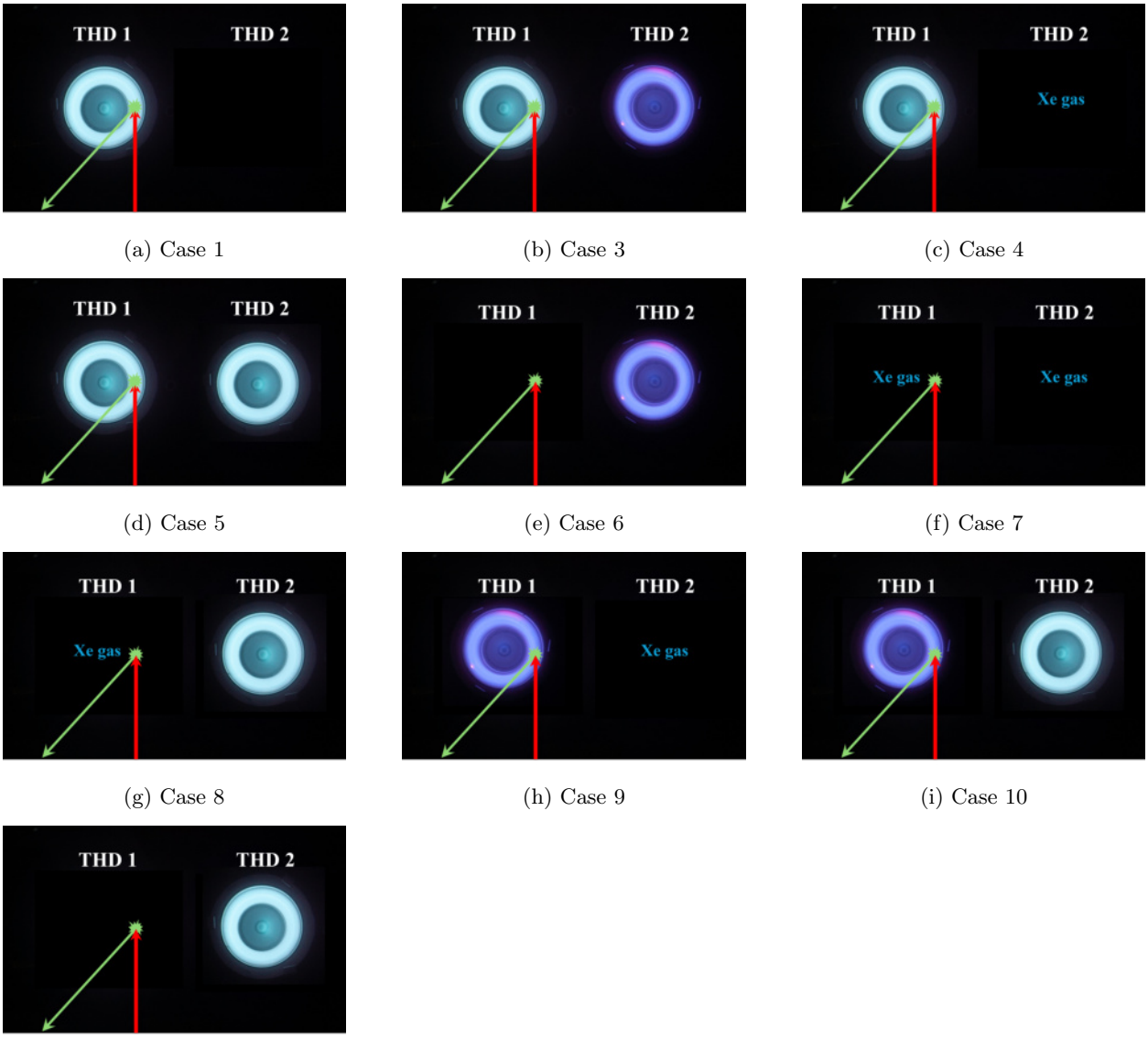

(a) Case 1 (b) Case 3 (c) Case 4

(d) Case 5 (e) Case 6 (f) Case 7

(g) Case 8 (h) Case 9 (i) Case 10

(j) Case 11

Figure 6: LIF experiment cases.

E. *Saturation of the optical transition*

LIF proves to be a reliable tool for assessing the Ion Velocity Distribution Function, as laser spectroscopy eliminates the need for in situ measurements that could potentially contaminate the plasma plume or alter the plasma equilibrum. To accurately determine the ion VDF,[4] it's crucial to ensure that the Doppler-shifted spectral line remains unaffected by saturation broadening—an instrumental effect arising when laser power intensity exceeds certain limits. In his review, M. J. Goeckner explains that saturation occurs when the stimulated photon emission rate equals or exceeds the photon absorption rate and surpasses the spontaneous photon emission rate, resulting in broadening of the measured fluorescence line.[8]

The saturation of the metastable Xe^+ optical transition utilized in this study has been experimentally investigated. Throughout the optical path, laser power is significantly reduced from the laser diode output to the inner vacuum chamber. As depicted in figure 3, a power meter is positioned at the end of the optical path, in front of the chamber window on the air side. An attenuation percentage of 10% is factored in to compute the final laser power in the measurement volume.

$$P_f = 2\alpha\beta\frac{P_{probed}}{\pi\phi_{laser}^2/4}$$

Here, P_f represents the final power density exciting Xe^+, α and β denote the attenuation coefficients of the lens and vacuum chamber window, P_{probed} indicates the probed power measured by the power meter, and ϕ_{laser} stands for the beam diameter. The factor 2 accounts for the chopper attenuation.

The laser power in the measurement volume was varied from 5mW to 40mW. Subsequently, the LIF signal was calculated by integrating the measured line profile. Figure 7 illustrates the LIF signal against laser power density. The signal exhibits a linear increase from 0 up to approximately 12 mW. Beyond this threshold, the evolution is no longer linear, marking the onset of saturation. Based on the trend of the LIF signal, saturation appears to occur at approximately 12 mW under our conditions at $x = 0$ mm. Consequently, to preserve the fluorescence lineshape integrity, 12 mW was consistently maintained for measurements throughout this study.

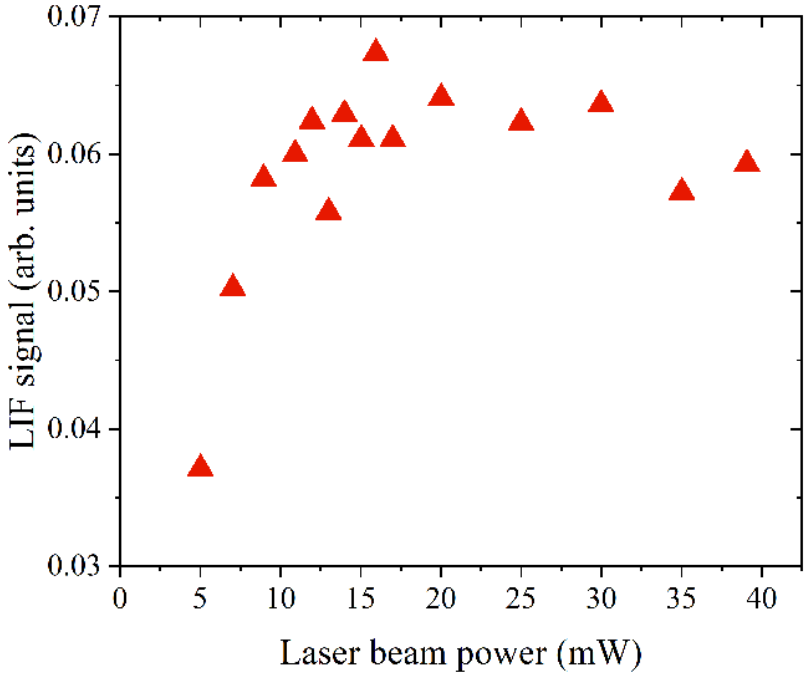

Figure 7: 834.9 nm metastable Xe+ optical transition saturation curve.

III. Xe II axial spectral distribution function

In this section, we will review measurements from the above conditions, in section II.D. Each case result is gathering three spectral acquisitions and have been adjusted to rebuild the entire profile. The LIF spectral profile images the Xe^+ ion VDF based on wavelenght swipe. The unit of the horizontal axis is the velocity unit here instead of the wavelength unit to directly access the ion most probable velocity. The axis unit has been converted using the Doppler shift formula. The laser range used to probe Xe^+ ion velocity profile extends from 834.9527 nm to 835.005 nm, according to equation 2. The Doppler shift corresponds to a particle velocity range of 0 km/s to 18 km/s.

The measured LIF spectra exhibit the standard Gaussian-like shape for a Hall thruster plume. Results have been normalized based on the red-infrared laser power and are compared on figure 9. Moreover, cases with a XeII ion detection are gathered and being compared in the graph figure 11.

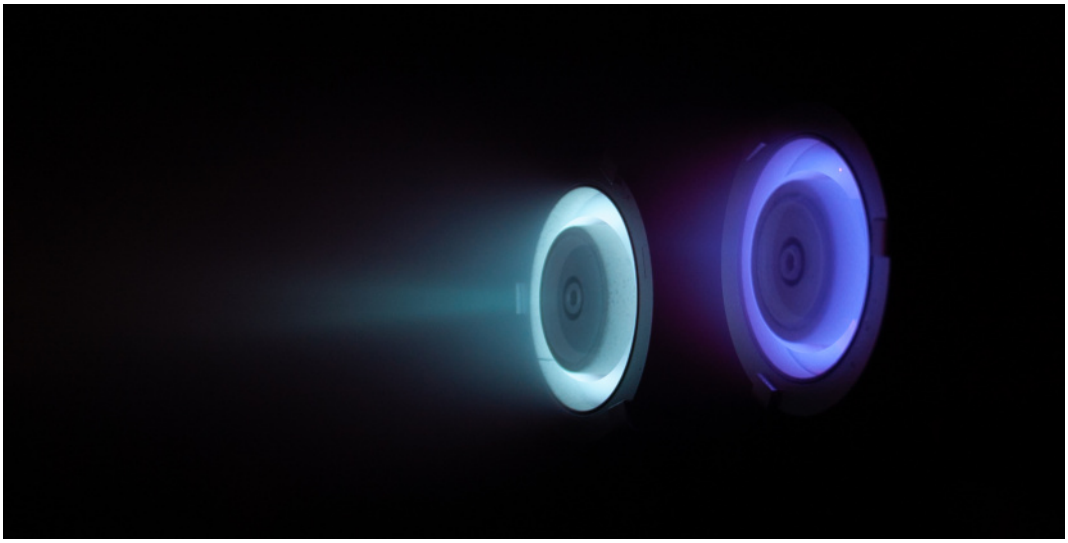

Figure 8: Photography of a cluster of two ISCT100 Hall thrusters firing with xenon (left) and krypton (right).

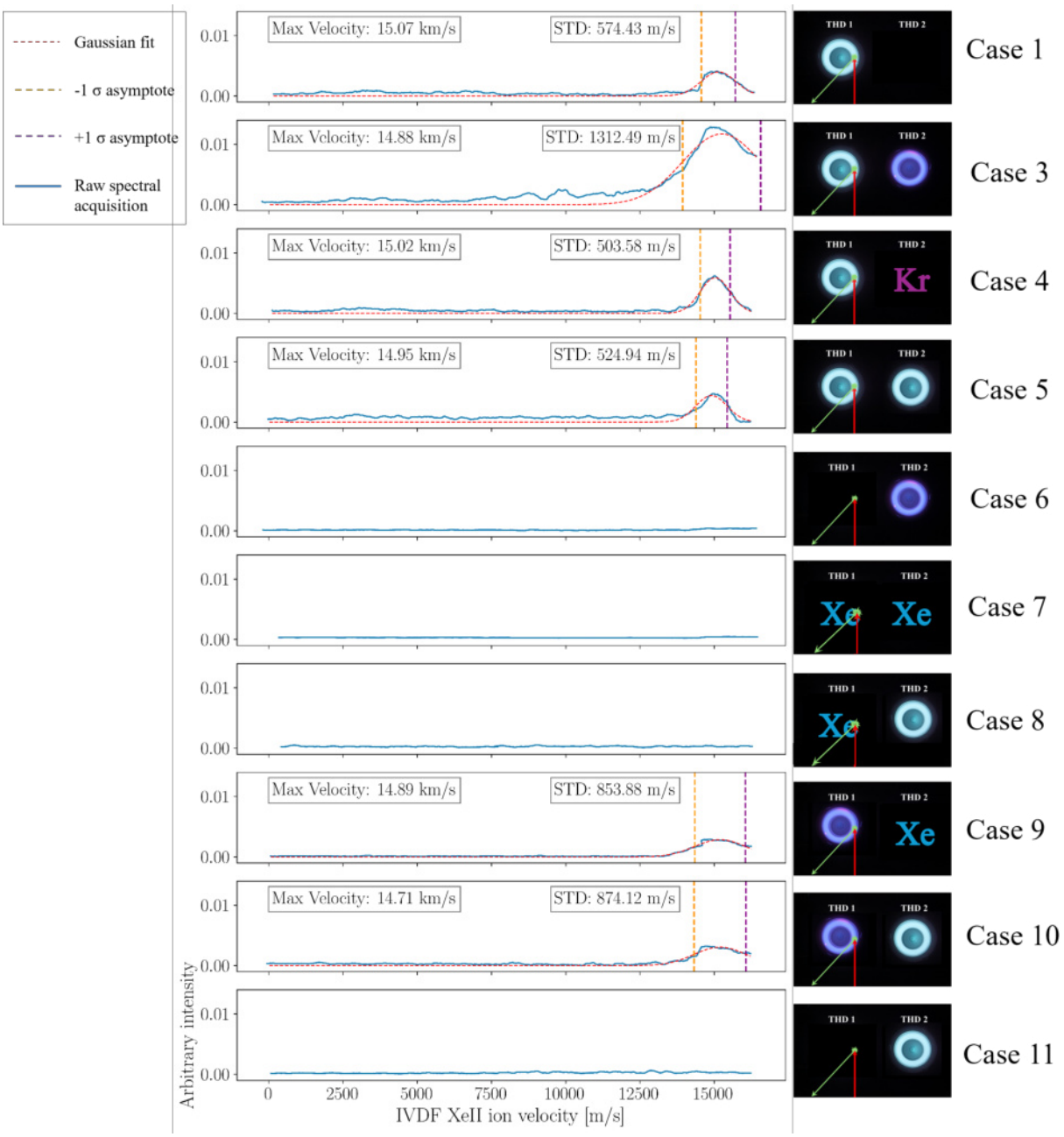

Figure 9: LIF results, showing IVDF for all cases. A peak detection is presented on each graph with its standard deviation.

This section is reviewing case results from figure 9. On condition one, only THD 1 is operating and is fed with xenon. This is the single-thruster reference case. A velocity peak is reached at 15.07 km/s, which is lesser than the expected V_{max} of 17.1 km/s from equation 1. Hence, energy is lost due to ionization, wall-plasma interaction, collisions, dispersions and beam divergence. Regarding the IVDF, a Gaussian fit curve is used to determine the mean value and the standard deviation (STD). A moderately high STD of +/- 574 m/s is noticed. The velocity peak is notable but not extremely broad.

Next graph, both thrusters are operating respectively with xenon and krypton. The XeII ion population is broader at 14.88 km/s resulting in the highest STD of +/- 1312 m/s. This plot is unexpected as it seems to show more fast ions gathered around the peak velocity, compared to case one. Case 1 and 2 aren't supposed to present such difference. This might results from a different operation or abnormal measurement.

On case four, one thruster is working with xenon with krypton gaz (KrI) injected in the THD2. The velocity peak is 15.02 km/s, STD is broadening to +/- 504 m/s. The peak is distinct but narrower than when both thrusters are operational with krypton, indicating more controlled ion velocity distribution.

Following on case 5, both thrusters are operating with xenon. Ion velocity peak is reached at 14.95 km/s with a STD of +/- 525 m/s. Similar to condition 3 but with xenon in THD2, resulting in a lower STD compared to dual thruster operation with xenon.

From case 6 to 8 with case 11, panels show minimal activity with no significant peaks, indicating that the probed THD were off. Case 6 is expected with no xenon injected in neither THD1 or THD2. Case 7 were also expected without signal as no ionization is generated. However case 8 and 11 are surprisingly signaless, despite xenon injection and a plasma created in THD2. This serves as a control condition, confirming that any detected ion activity in other panels is due to the presence of a plasma activity in THD1.

Case 9 presents one thruster operating with krypton and the other turned off with xenon gas injected. A ion population is detected at 14.89 km/s with a STD of +/- 854 m/s. The presence of a moderate STD and a distinct peak suggests interaction between the different ionized gases. This experiment is really relevant and shows that XeII ion are produced in the THD1 krypton plasma vinicity with Xe gaz THD2.

Finally, case 10, thrusters are both operational, with one using xenon THD2 and the other krypton THD1. Velocity peak reached at 14.71 km/s and a STD of +/- 874 m/s. This higher STD compared to case 9 suggests increased interaction and possibly a more complex ion velocity distribution due to the simultaneous use of thruster, despite the fact that case 11 confirms that XeII from THD2 remain unseen.

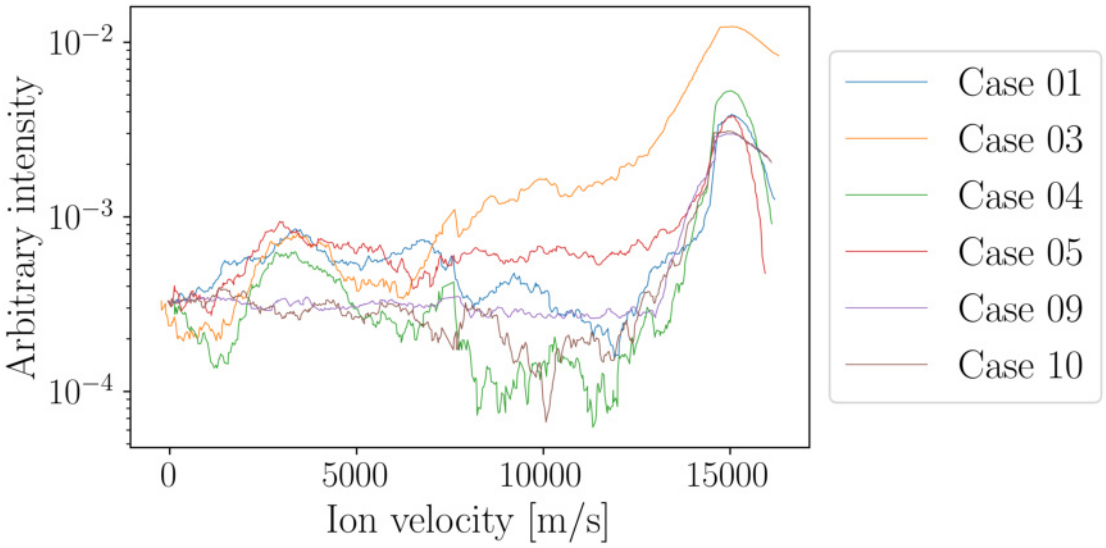

Figure 10: IVDF cases plotted in logarithm scale.

From figure 9, higher STDs generally correlate with configurations involving both thrusters being operational, particularly with different propellants (xenon and krypton). Lower STDs are observed when only one thruster is operational. This is just supposition as we cannot relate on laser intensity. Moreover, ISCT 100 thruster operation is not reliable as thruster firing is inconstant from one day to another.

From figure 10, the data processing suggest a lite secondary ion population at $\approx 2.7 km/s$ for case 1, 3, 4 and 5 which are the only cases with THD1 operating with xenon plasma. Those might come from freshly ionized Xe ions between ionization and acceleration region.

Figure 11 reveals that XeII ion energy remains constant through out all cases and conditions. The absence of peaks indicates no ion activity, as expected when the THD1 is off.

Krypton, when used alone or in combination with xenon, tends to produce broader standard deviation on XeII ion IVDF, indicating a larger distribution of ion velocities. This could be due to krypton's different ionization characteristics, which result in higher energy ions, but again as it was previously said, this statement is just supposition as we cannot relate on laser intensity.

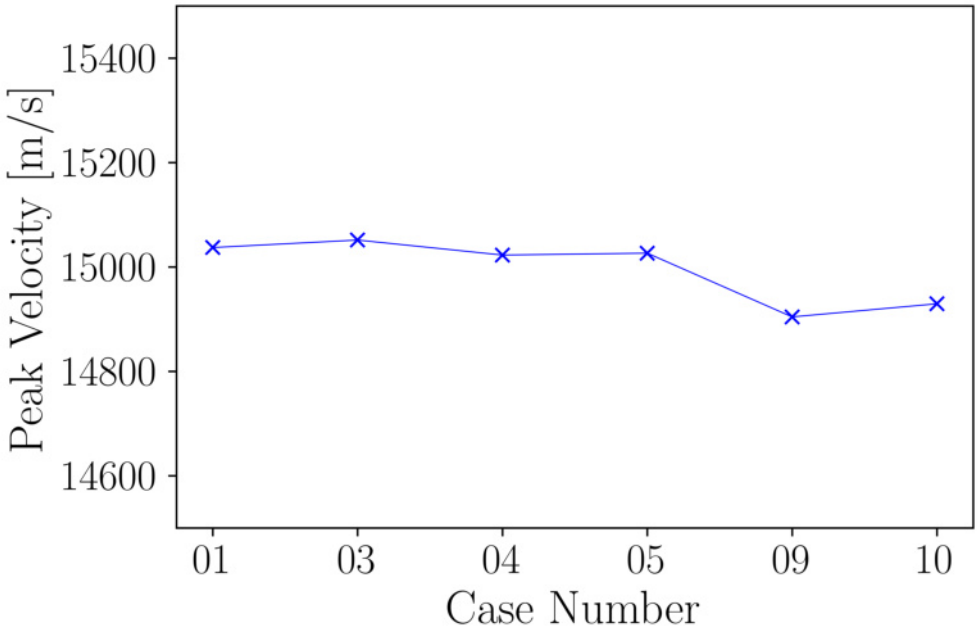

Figure 11: Blue graph shows the XeII peak velocity for cases which have register fluorescence signal.

Operating both thrusters simultaneously results in higher STDs and broader velocity distributions, suggesting more complex interactions and higher energy ions. This seems to be particularly enhanced when different propellants are used. Single thruster operation seems to yield more controlled and narrower velocity distributions, as indicated by lower STDs.

The data seem to highlight the system's sensitivity to different operational configurations and propellants, which is crucial for optimizing ion thruster performance and understanding ion dynamics in varying conditions. However, those remarks should be taken cautionly, knowing that laser intensity and thruster operations vary a lot during a day of experiment and from one day to another.

During this study, a careful attention have been brought on thruster stability and consistency in order to perform clearest and coherent measurement with LIF. Figure 12, presents discharge current measurements and standard deviations for each cases where ion activity have been detected. Each discharge current frequency are highlighted on figure 13. As usual, the Breathing Mode is standing out from other frequency peaks between 10 to 20 kHz. Moreover, the Transit Time Instabilities is also present in a lower intensity around 200 kHz.

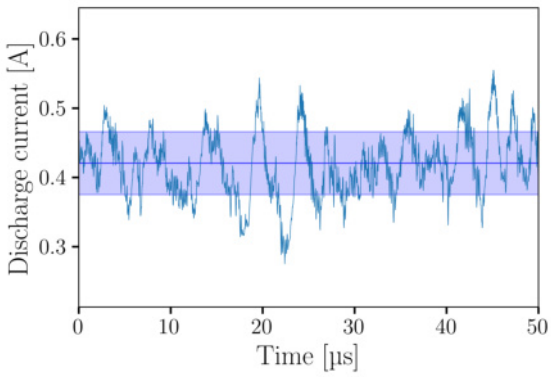

(a) Case 1

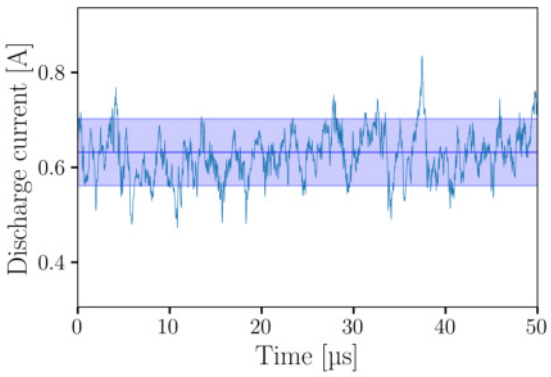

(b) Case 3

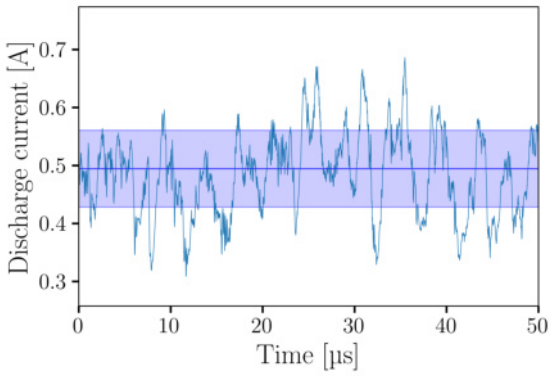

(c) Case 4

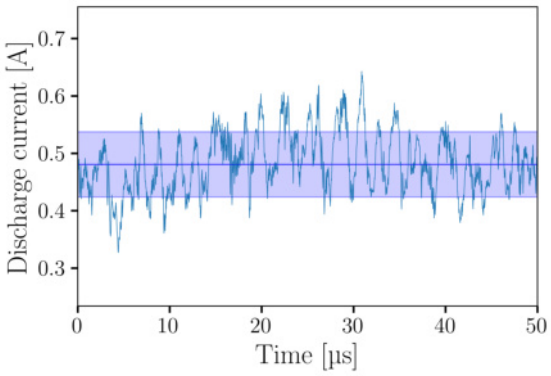

(d) Case 5

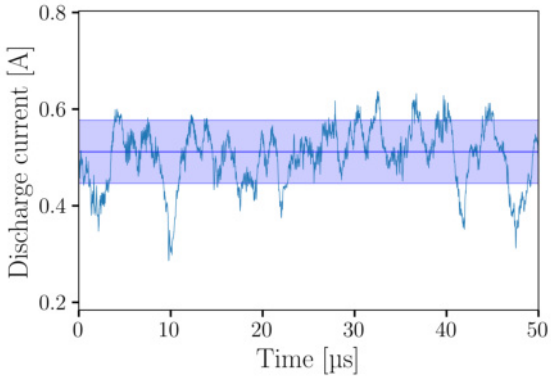

(e) Case 9

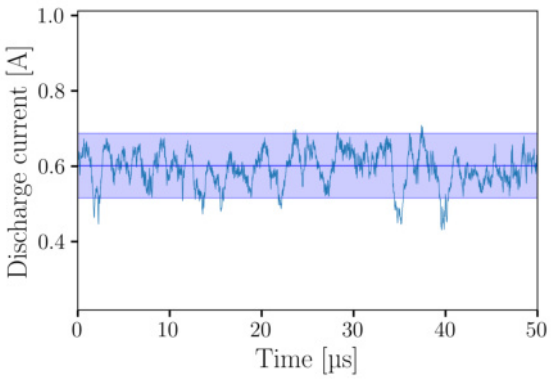

(f) Case 10

Figure 12: THD 1 current discharge and standard deviation represented in blue region.

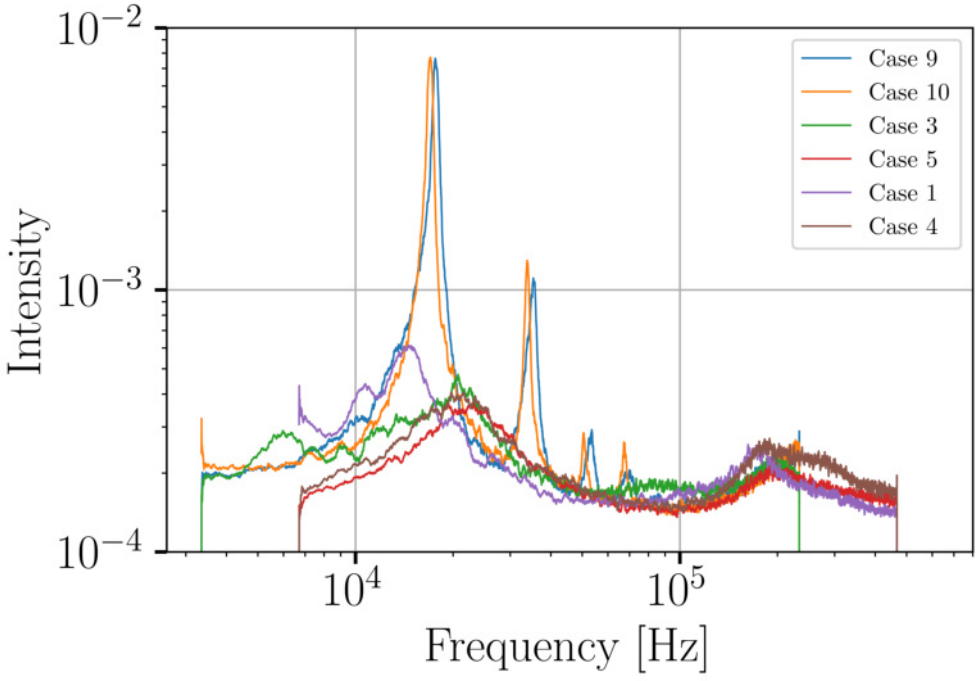

Figure 13: Frequency analysis of discharge current.

IV. Conclusion

This study marks the inaugural exploration of Hall thruster plume interaction in a cluster configuration utilizing LIF spectroscopy on ions. The experiments focused on metastable Xe^+ ions within the plasma plume generated by two low-power miniature ISCT100 Hall thrusters arranged in a cluster configuration with a single cathode, operating with krypton. Both xenon and krypton were employed as propellant gases for anode subsystems. Initial findings reveal phenomena of invasion and penetration, as particles originating from one thruster are detected within the plume of neighboring thrusters. Furthermore, the figure demonstrates that dual thruster operation, especially with different propellants, could lead to more complex and more energetic ion velocity distributions, whereas single thruster operation results in more controlled ion activity. This insight is valuable for the design and optimization of ion thrusters in practical applications.

Acknowledgments

C. Royer benefits from a CNES/Exotrail Ph.D. grant. This study was performed within the framework of the ORACLE joint-laboratory program. I would like to thank singularly Alexis Lecervoisier for his support.

References

[1]Brian E Beal, Alec D Gallimore, and William A Hargus Jr. Effects of cathode configuration on hall thruster cluster plume properties. *Journal of Propulsion and Power*, 23(4):836–844, 2007.

[2]Jean-Pierre Boeuf. Tutorial: Physics and modeling of hall thrusters. *Journal of Applied Physics*, 121(1):011101, 2017.

[3]Sarah E Cusson, Marcel P Georgin, Horatiu C Dragnea, Ethan T Dale, Vira Dhaliwal, Iain D Boyd, and Alec D Gallimore. On channel interactions in nested hall thrusters. *Journal of Applied Physics*, 123(13):133303, 2018.

[4]MJ Goeckner and J Goree. Laser-induced fluorescence measurement of plasma ion temperatures: Corrections for power saturation. *Journal of Vacuum Science & Technology A: Vacuum, Surfaces, and Films*, 7(3):977–981, 1989.

[5]Thibault Hallouin and Stéphane Mazouffre. Far-field plume characterization of a 100-w class hall thruster. *Aerospace*, 7(5):58, 2020.

[6]Robert B Lobbia and Alec D Gallimore. Performance measurements from a cluster of four hall thrusters. In *30th International Electric Propulsion Conference, Florence, Italy*, 2007.

[7]Stéphane Mazouffre. Laser-induced fluorescence diagnostics of the cross-field discharge of hall thrusters. *Plasma Sources Science and Technology*, 22(1):013001, 2012.

[8]Stéphane Mazouffre. Laser-induced fluorescence spectroscopy applied to electric thrusters. *Von Karman Institute for Fluid Dynamics, STO-AVT-VKI Lecture series 263*, pages p–10, 2016.

[9]Stéphane Mazouffre and Lou Grimaud. Characteristics and performances of a 100-w hall thruster for microspacecraft. *IEEE Transactions on Plasma Science*, 46(2):330–337, 2018.

[10]George-Cristian Potrivitu, Romain Joussot, and Stéphane Mazouffre. Anode position influence on discharge modes of a lab6 cathode in diode configuration. *Vacuum*, 151:122–132, 2018.

[11]Clemence Royer, T Hallouin, AE Vinci, and S Mazouffre. A lif study on the plasma plume of a cluster of two 100 w hall thrusters. In *37th International Electric Propulsion Conference*, 2022.

[12]Alfio E. Vinci and Stéphane Mazouffre. Laser-induced fluorescence spectroscopy on xenon atoms and ions in the magnetic nozzle of a helicon plasma thruster. *submitted to Plasma Source Science and Technology, 2022*, 2022.

[13]Mitchell LR Walker and Alec D Gallimore. Hall thruster cluster operation with a shared cathode. *Journal of Propulsion and Power*, 23(3):528–536, 2007.

[14]Mitchell LR Walker and Alec D Gallimore. Performance characteristics of a cluster of 5-kw laboratory hall thrusters. *Journal of Propulsion and Power*, 23(1):35–43, 2007.